Unified description of charmonium suppression in a quark-gluon plasma medium at RHIC and LHC energies

Captain R. Singh,[1] P. K. Srivastava,[2,*] S. Ganesh,[1] and M. Mishra[1,†]
[1]*Department of Physics, Birla Institute of Technology and Science Pilani, Pilani - 333031, India*
[2]*Department of Physics, Indian Institute of Technology Roorkee, Roorkee - 247667, India*
(Received 25 May 2015; published 24 September 2015)

Recent experimental and theoretical studies suggest that the quarkonium suppression in a thermal QCD medium created in heavy ion collisions is a complex interplay of various physical processes. In this article we put together most of these processes in a unified way to calculate the charmonium survival probability (nuclear modification factor) at energies available at Relativistic Heavy Ion Collider (RHIC) and Large Hadron Collider (LHC) experiments. We include shadowing as the dominant cold-nuclear-matter effect. Further, gluonic dissociation and collision damping are included, which provide width to the spectral function of charmonia in a thermal medium and cause the dissociation of charmonium along with the usual color screening. We include color screening by using our recently proposed modified Chu–Matsui model. Furthermore, we incorporate the recombination of uncorrelated charm and anticharm quarks for the regeneration of charmonium over the entire temporal evolution of the QGP medium. Finally, we do a feed-down correction from the excited states to calculate the survival probability of charmonium. We find that our unified model suitably and simultaneously describes the experimental nuclear modification data of J/ψ at RHIC and LHC.

DOI: 10.1103/PhysRevC.92.034916 PACS number(s): 12.38.Mh, 12.38.Gc, 25.75.Nq, 24.10.Pa

I. INTRODUCTION

The physical picture of quarkonium dissociation in a thermal medium has undergone theoretical and experimental refinements over the last decade [1]. Heavy quarkonium ($J/\psi, \Upsilon$, etc.) suppression is considered as the most classical observable of QGP formation in heavy ion collision experiments. This is because the heavy mass scale ($m = 3.1$ GeV for J/ψ and $m = 9.2$ GeV for Υ) makes these system possible for analytical treatment theoretically. On the other side, decay of heavy quarkonia via a dileptonic channel leads to relatively clean signals which can be precisely measured experimentally. Until the mid-2000s, Debye screening was thought to be the only possible mechanism for the anomalous suppression of charmonium (J/ψ) and bottomonium (Υ) [2] in a QGP medium. However, experimental results involve some puzzling features which defy explanations based on color screening alone [3–7]. The first such experimental result is the lower suppression at midrapidity than forward rapidity observed at the Relativistic Heavy Ion Collider (RHIC) and also at the Large Hadron Collider (LHC) [6,7] which is in contradiction to the color-screening scenario (because color screening predicts a larger suppression at a higher-density region of plasma which is actually the midrapidity). Second, such an experimental result is the same amount of charmonium suppression at SPS and RHIC energies for the same number of participants [4]. Although the available energy spans over two orders of magnitude in moving from the CERN Super Proton Synchrotron (SPS) to the LHC, the amount of charmonium suppression is found to be similar. Regeneration of charmonia in QGP through the recombination of c and $\bar{c}$ quarks is believed to be the main reason for this experimental observation. The third experimental observation is the suppression pattern in forward and backward rapidity in d-Au collisions at RHIC. A suppression is observed at forward rapidity (in the d-going direction) and an enhancement at backward rapidity (in the Au-going direction) [8]. This result suggests the importance of charmonium breakup effects in nuclear matter in the final stages of the collision, apart from the usual cold-nuclear-matter effects in the initial stage. All these experimental observations suggest that the charmonium suppression in QCD plasma is not the result of a single mechanism but is a complex interplay of various physical processes.

On the theoretical side, the development in thermal field theory shows that the static potential between two heavy quarks placed in a QCD medium consists of two parts [9,10]. It is the first part which represents the standard time-independent Debye-screened potential (earlier it was thought that the Debye-screened potential is only the dominant part in the heavy-quark potential, based on which one can understand the dissociation of quarkonia in QGP). The second part of potential, other than the standard Debye-screened part, is imaginary and, in the limit of $t \to \infty$, represents the thermal decay width induced by Landau damping of the low-frequency gauge fields that mediate interactions between two heavy quarks [9]. Later Brambilla *et al.* [11] showed that thermal width can also originates from singlet-to-octet transition of heavy meson resonance due to gluonic interaction apart from the imaginary part of the gluon self-energy. In a QGP, gluons can collide with a color-singlet heavy quarkonium, leading to its dissociation [12]. Dissociation by the absorption of a single gluon is allowed because the color-octet final state of a free quark and antiquark can propagate in the colored QGP medium, in contrast to the colorless hadronic medium. One of the earlier treatments of the dissociation of heavy quarkonium by the absorption of an $E1$ gluon (where $E1$ is the lowest

*prasu111@gmail.com
†madhukar.12@gmail.com

electric mode for the spin-orbital wave function of gluons) was carried out by Peskin and Bhanot [13,14]. Therefore, the dissociation of quarkonia does not happen only due to Debye screening but can also occur by the gluonic dissociation and the collisional damping (Landau damping) as well.

The production of charmonium in nucleon-nucleon collisions is also an involved process [15]. The charmonia production process in elementary hadronic collisions, e.g., $p+p$ collisions, begins with the formation of a $c\bar{c}$ pair; this pair can then either lead to open charm production or subsequently bind to form a charmonium state (about 10% for all charmonia) [16]. The dominant high-energy production mechanism for charmonia is gluon-gluon fusion. Based on the scales involved, the production process of charmonia is believed to be factorizable into two parts: a charm and anticharm quark produced through nucleon-nucleon collision is a perturbative QCD process [15]. However, the formation and evolution of this pair into a meson is governed by nonperturbative QCD. Hence, heavy-quarkonia provide a unique laboratory which can explore the interplay of perturbative and nonperturbative QCD effects. A variety of theoretical approaches has been proposed in the literature to calculate the heavy quarkonium production in nucleon-nucleon collisions [17–22]. Nonrelativistic QCD (NRQCD) [17,18] and fragmentation approaches [19,20] are the two theoretical methods based on QCD which are being used in most of the quarkonium production and suppression models. However, the heavy quarkonium production mechanism is still a topic of intense debate.

The heavy-quarkonia production processes, in the case of nucleus-nucleus collisions, are significantly affected by the nuclear environment [23]. These effects are known as cold-nuclear-matter (CNM) effects. In most of the literature, three CNM effects are considered. The first and dominant CNM effect in the case of quarkonium production is shadowing. Change in the parton distribution function in the nucleus which control the initial parton behavior and strongly depends on the collisional kinematics (in the small-x region the nuclear parton distribution function is clearly suppressed compared to that of nucleon) is known as shadowing [24]. The shadowing causes the production cross section to become less in the A-A case than that of pure N-N collisions. The second CNM contribution is known as the Cronin effect [25,26]. It describes the initial gluon multiscattering with the neighboring nucleons presented in the nucleus prior to hard scattering and quarkonium formation. This results in the broadening of transverse momentum distribution of produced charmonia. Nuclear absorption [27] is another CNM contribution to the charmonium production. The interaction between charmonia and the primary nucleons leads to the normal suppression of charmonia. Nuclear absorption is the dominant CNM effect at lower energies. However, the cross section for nuclear absorption decreases with the increase in energy [28].

Recently, it was proposed that recombination of initially uncorrelated c and $\bar{c}$ quarks in QGP can also regenerate the charmonia states [29–35]. The calculation of regeneration of charmonium is based on the statistical hadronization model [29,30] and the kinetic model in which J/ψ production is described via dynamical melting and regeneration over the whole temporal evolution of the QGP [31–33,35]. Some transport calculations were also performed to calculate the number of regenerated J/ψ [36,37]. At lower energies, this contribution is very low and almost negligible because of the lower number of initially produced charm quarks. However, at the higher energies of the RHIC and LHC, the regeneration factor becomes important. Thus J/ψ whose suppression is actually proposed as a signal to confirm the existence of the quark-gluon plasma earlier can also turn out to provide an extremely useful probe of the QCD medium created at heavy-ion-collision experiments.

In this article we present a unified model which includes most of the above dissociation as well as production (recombination) processes to finally calculate the survival probability of J/ψ in a QGP medium. We constructed this model based on the kinetic approach whose original ingredients were given by Thews *et al.* [33–35]. In this approach, there are two terms written on the basis of the Boltzmann kinetic equation. First term, which we call the dissociation term, includes dissociation processes such as gluonic dissociation and collisional damping. The second term (formation term) provides the (re)generation of J/ψ due to the recombination of charm-anticharm quarks. These two terms compete over the entire temporal evolution of the QGP and at freeze-out temperature we get the multiplicity of the surviving J/ψ. To include the gluonic dissociation we got help from a model developed by Nendzig and Wolschin [38] and later used by two of the authors [39]. The thermal width due to collisional damping is calculated based on the thermal field theory, as discussed by Laine *et al.* [9]. We also include the shadowing effect to incorporate the CNM effect properly into the production process. We consider color screening as a dissociation process of charmonium acting until the formation of charmonium bound states followed by gluonic dissociation along with collisional damping. It means that the color screening is active at the initial times of medium evolution when the temperature is high enough to melt down the charmonium states. Later, the dissociation probability by color screening diminishes rapidly and becomes zero at lower temperatures (for times larger than the quarkonium-formation time). To include the dissociation of J/ψ due to Debye screening (color screening) in the QCD plasma, we used a new model constructed by two of the authors based on the color screening in the QGP [40,41]. In this color-screening model we use the quasiparticle (QPM) equation of state (EOS) to describe the basic partonic properties of the QGP phase. To define the dynamics of the system created in the heavy ion collisions, we use $(1+1)$-dimensional viscous hydrodynamics. We include only the shear viscosity and neglect the bulk viscosity. We also suitably incorporate the overall feed-down correction from the higher charmonium states (χ_c and $\psi^{'}$) to the charmonium (J/ψ).

II. MODEL FORMALISM

The abundance of charm quarks, antiquarks, and their bound state, i.e., charmonia states (J/ψ, χ_c, $\psi^{'}$, etc.), is governed by a simple master equation involving two reactions:

the formation reaction and the dissociation reaction. Thus the time evolution of the number of bound charmonium states in the deconfined region can be written as [33]

$$\frac{dN_{J/\psi}}{d\tau} = \Gamma_{F,nl} N_c N_{\bar{c}} [V(\tau)]^{-1} - \Gamma_{D,nl} N_{J/\psi}. \quad (1)$$

In the equation above, the first term on the right-hand side represents the formation term by recombination of uncorrelated charm quark and antiquark. The second term on the right-hand side is the dissociation term of charmonium. $\Gamma_{D,nl}$ and $\Gamma_{F,nl}$ are the dissociation width and recombination reactivity corresponding to the dissociation and regeneration of charmonia, respectively. It is important here to mention that the units of $\Gamma_{D,nl}$ are GeV or fm^{-1}. However, the recombination reactivity $\Gamma_{F,nl}$ has units of fm^2 or GeV^{-2}. It only changes into fm^{-1} or GeV when it is multiplied by the inverse of the system volume $[V(\tau)]^{-1}$. N_c, $N_{\bar{c}}$, and $N_{J/\psi}$ are the numbers of produced charm, anticharm, and J/ψ, respectively. At the initial time, we have taken $N_c = N_{\bar{c}} = N_{c\bar{c}}$. When the total number of regenerated charmonia is less than the initial number of $N_{c\bar{c}}$, one can obtain the analytical solution of Eq. (1) as follows [34]:

$$N_{J/\psi}(\tau_f,b) = \epsilon(\tau_f)\Bigg[N_{J/\psi}(\tau_0,b) + N_{c\bar{c}}^2 \int_{\tau_0}^{\tau_f} \Gamma_{F,nl} \times [V(\tau)\epsilon(\tau)]^{-1} d\tau\Bigg], \quad (2)$$

where τ_0 is the initial thermalization time of the QGP and τ_f is the lifetime of the QGP. $N_{J/\psi}(\tau_0,b)$ is the initial multiplicity and $N_{J/\psi}(\tau_f,b)$ is the final number of survived J/ψ mesons. The variables used in Eq. (2), $\epsilon(\tau_f)$ and $\epsilon(\tau)$, are the suppression factors which can be obtained by using the following expressions:

$$\epsilon(\tau_f) = \exp\left[-\int_{\tau_0}^{\tau_f} \Gamma_{D,nl} d\tau\right], \quad (3)$$

and

$$\epsilon(\tau) = \exp\left[-\int_{\tau_0}^{\tau} \Gamma_{D,nl} d\tau\right]. \quad (4)$$

We have defined $\Gamma_{D,nl}$ as the net sum of collisional damping reaction rate ($\Gamma_{\text{damp},nl}$) and gluonic dissociation reaction rate ($\Gamma_{gd,nl}$) of charmonia in QGP, given as

$$\Gamma_{D,nl} = \Gamma_{gd,nl} + \Gamma_{\text{damp},nl}. \quad (5)$$

The initial time τ_0 is taken as the formation time required for charmonium formation and where the dissociation due to color screening becomes zero. τ_0 is taken as 0.89,2.0 and 1.5 for J/ψ, χ_c and $\psi^{'}$, respectively [42].

A. Gluonic dissociation and collisional damping

The dissociation of the $c\bar{c}$ bound state due to gluonic dissociation along with collisional damping in a QGP medium was formulated by Wolschin *et al.* [12,38]. Here we briefly discuss these dissociation mechanisms.

1. Collisional damping

To determine the collisional dissociation and gluonic dissociation rate, we get help from effective-potential models. In our work, we use the singlet potential for c-$\bar{c}$ bound state in the QGP as follows [38]:

$$V(r,m_D) = \frac{\sigma}{m_D}(1 - e^{-m_D r}) - \alpha_{\text{eff}}\left(m_D + \frac{e^{-m_D r}}{r}\right) - i\alpha_{\text{eff}} T \int_0^{\infty} \frac{2z dz}{(1+z^2)^2}\left(1 - \frac{\sin(m_D r z)}{m_D r z}\right), \quad (6)$$

where the first and second term on the right-hand side is the string term and the columbic term, respectively. The third term on the right-hand side is the imaginary part of the heavy-quark potential. In Eq. (6),

(1) σ is the string-tension constant between the $c\bar{c}$ bound state, given as $\sigma = 0.192$ GeV^2.
(2) m_D is the Debye mass, $m_D = T[4\pi\alpha_s^T(\frac{N_c}{3} + \frac{N_f}{6})]^{1/2}$, and α_s^T is a coupling constant at hard scale, as it should be $\alpha_s^T = \alpha_s(2\pi T) \leqslant 0.50$ [38]. For charmonia we found $\alpha_s^T \simeq 0.25$. Here we considered $N_c = 3$, $N_f = 3$, and the evolution of temperature T as the function of time τ and impact parameter b [39].
(3) α_{eff} is the effective coupling constant and depends on the strong coupling constant at the soft scale $\alpha_s^s = \alpha_s(m_c\alpha_s/2) = 0.4725$, given as $\alpha_{\text{eff}} = \frac{4}{3}\alpha_s^s$.

The decay rate, $\Gamma_{\text{damp},nl}$, accounts for collisional damping by the QGP partons. The imaginary part of potential causes the collisional damping (also termed as Landau damping in the literature). Therefore, the decay rate can be obtained via a first-order perturbation by folding of imaginary part of the potential with the radial wave function and is given by;

$$\Gamma_{\text{damp},nl} = \int [g_{nl}(r)^{\dagger}[\text{Im}(V)]g_{nl}(r)]dr, \quad (7)$$

here, $g_{nl}(r)$ is the charmonium wave function. Corresponding to different values of n and l, we obtained the wave functions for $1S(J/\psi)$, $1P(\chi_c)$, and $2S(\psi^{'})$ by solving the Schrödinger equation.

2. Gluonic dissociation

In a QGP, gluons can collide with a color-singlet heavy quarkonium leading to its dissociation. The ultrasoft gluon makes the color-singlet object to a color-octet object which further dissociates at the time of freeze-out. The cross section for this gluonic dissociation process can be given as follows [38]:

$$\sigma_{d,nl}(E_g) = \frac{\pi^2\alpha_s^{\mu} E_g}{N_c^2}\sqrt{\frac{m_c}{E_g + E_{nl}}}\left(\frac{l\left|J_{nl}^{q,l-1}\right|^2 + (l+1)\left|J_{nl}^{q,l+1}\right|^2}{2l+1}\right), \quad (8)$$

where $J_{nl}^{ql'}$ is the probability density obtained by using the singlet and octet wave functions

$$J_{nl}^{ql'} = \int_0^\infty dr r g_{nl}^*(r) h_{ql'}(r), \tag{9}$$

and

(1) $m_c = 1.3$ GeV is the mass of the c and $\bar{c}$.
(2) $\alpha_s^u \simeq 0.59$ [38] is the coupling constant, scaled as $\alpha_s^u = \alpha_s(\alpha_s m_c^2/2)$.
(3) E_{nl} is energy eigenvalues corresponding to the charmonium wave function $g_{nl}(r)$.
(4) the radial wave function $h_{ql'}(r)$ has been obtained by solving the Schrödinger equation with the octet potential $V_8 = \alpha_{\text{eff}}/8r$ and the value of q is determined from energy conservation; $q = \sqrt{m_c(E_g + E_{nl})}$.

The Schrödinger equation has been solved by taking a 10^4-point logarithmically spaced finite spatial grid and solving the resulting matrix eigenvalue equations [39]. For the octet modeling the potential is repulsive, which implies that the quark and antiquark can be far away from each other. To account for this, the finite spatial grid is taken over a very large distance, namely 10^2, as an approximation for infinity. The octet wave function corresponding to large $c\bar{c}$ distance has negligible contribution to the gluonic dissociation cross section.

To obtain the gluonic decay rate $\Gamma_{gd,nl}$, we calculated the mean of gluonic dissociation cross section by taking its thermal average over the Bose–Einstein distribution function for gluons. Thus the rate of gluonic dissociation can be written as

$$\Gamma_{gd,nl} = \frac{g_d}{2\pi^2} \int_0^\infty \frac{dp_g p_g^2 \sigma_{d,nl}(E_g)}{e^{E_g/T} - 1}, \tag{10}$$

where $g_d = 16$ is the number of gluonic degrees of freedom. Equation (10) has been derived for idealized case where J/ψ is at rest in a thermal bath of gluons.

The total dissociation rate along with its components, i.e., gluonic dissociation and collisional damping decay rates versus temperature are shown in Fig. 1. This figure depicts that the decay rate of charmonia due to gluonic dissociation remains insignificant until $T = 0.250$ GeV and increases slowly beyond this temperature. However, the collisional damping decay rate contributes significantly throughout whole temperature range. The gluonic dissociation cross section for J/ψ versus gluon energy, E_g at temperatures $T = 0.170$ GeV and $T = 0.300$ GeV are also depicted in Fig. 2.

B. Regeneration via c and $\bar{c}$ quarks

The recombination reactivity $\Gamma_{F,nl}$ required in Eq. (2) is calculated by taking the thermal average of the product of the recombination cross section and the initial relative velocity between c and $\bar{c}$, $\langle \sigma_{f,nl} v_{\text{rel}} \rangle_{p_c}$ by using the modified Fermi–Dirac distribution function for charm quarks at temperature T as follows [35]:

$$\Gamma_{F,nl} = \frac{\int_{p_{c,\min}}^{p_{c,\max}} \int_{p_{\bar{c},\min}}^{p_{\bar{c},\max}} dp_c dp_{\bar{c}} p_c^2 p_{\bar{c}}^2 f_c f_{\bar{c}} \sigma_{f,nl} v_{\text{rel}}}{\int_{p_{c,\min}}^{p_{c,\max}} \int_{p_{\bar{c},\min}}^{p_{\bar{c},\max}} dp_c dp_{\bar{c}} p_c^2 p_{\bar{c}}^2 f_c f_{\bar{c}}}, \tag{11}$$

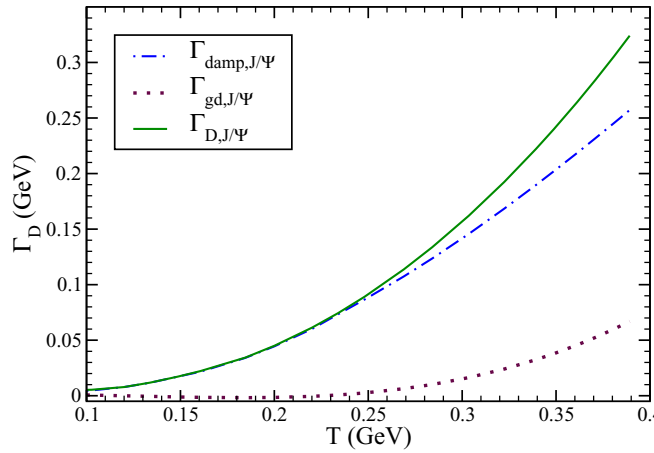

FIG. 1. (Color online) Variation of total dissociation width with temperature along with its components, i.e., gluonic dissociation width and width due to collisional damping.

where p_c and $p_{\bar{c}}$ are the momentum of charm and anticharm quark, respectively. $f_{c,\bar{c}}$ is the modified Fermi–Dirac distribution function of charm and anticharm quark given as, $f_{c,\bar{c}} = \lambda_{c,\bar{c}}/(e^{E_{c,\bar{c}}/T} + 1)$, here $E_{c,\bar{c}} = (p_{c,\bar{c}}^2 + m_{c,\bar{c}}^2)^{1/2}$ is the energy of the charm and anticharm quark in the medium with mass $m_{c,\bar{c}} = 1.3$ GeV, and $\lambda_{c,\bar{c}}$ is their respective fugacity term [43]. We have calculated relative velocity of $c\bar{c}$ pair in the medium, given as

$$v_{\text{rel}} = \sqrt{\frac{\left(p_c^\mu p_{\bar{c}\mu}\right)^2 - m_c^4}{p_c^2 p_{\bar{c}}^2 + m_c^2\left(p_c^2 + p_{\bar{c}}^2 + m_c^2\right)}}. \tag{12}$$

The recombination cross section $\sigma_{f,nl}$ was obtained by using detailed balance from the dissociation cross section $\sigma_{d,nl}$ [33] as follows:

$$\sigma_{f,nl} = \frac{48}{36}\sigma_{d,nl}\frac{\left(s - M_{nl}^2\right)^2}{s\left(s - 4m_c^2\right)}. \tag{13}$$

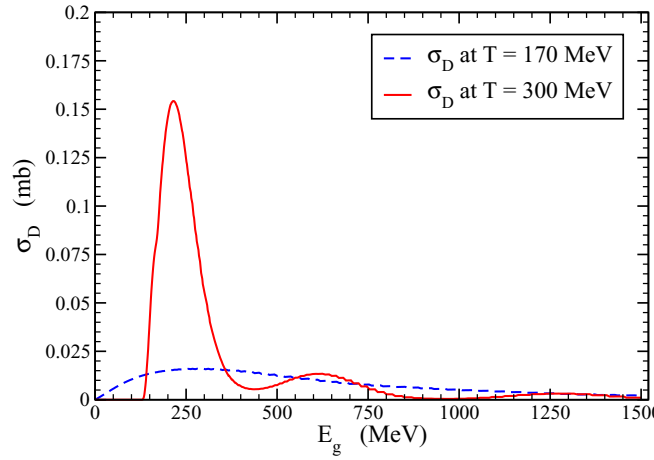

FIG. 2. (Color online) Variation of gluonic-dissociation cross section of J/ψ with respect to gluon energy E_g at $T = 0.170$ GeV and $T = 0.300$ GeV.

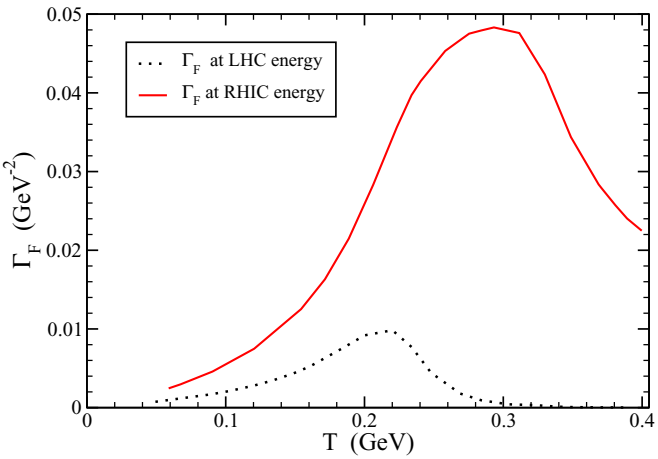

FIG. 3. (Color online) Variation of recombination reactivity with respect to temperature at RHIC ($\sqrt{s_{NN}} = 200$ GeV) and at LHC ($\sqrt{s_{NN}} = 2.76$ TeV).

Here, $M_{nl} = (M_{J/\psi}, \chi_c, \psi^{'})$ is the mass of the charmonium states. $s = (p_1 + p_2)^2$ is related to the center-of-mass energy of the $c\bar{c}$ pair with p_1 and p_2 as four-momentum of the c and $\bar{c}$ quarks, respectively.

Γ_F for J/ψ versus temperature T at both RHIC and LHC energies are shown in Fig. 3. Its value at RHIC energies is found to be larger as compared with the corresponding number at LHC energies. This trend may be due to the low initial momentum of the charm and anticharm quarks which participate in the J/ψ formation at RHIC compared to LHC. It is also obvious from the above figure that the recombination reactivity Γ_F at LHC increases with temperature, attains a maximum value at around $T = 0.225$ GeV, and vanishes at $T = 0.300$ GeV. However, at RHIC energies it peaks at $T = 0.300$ GeV and remains finite even at the temperature $T = 0.400$ GeV.

C. Inputs to the model

In this section we provide the prescriptions to calculate various inputs which have been used in our model. $N_{J/\psi}(\tau_0)$ and $N_{c\bar{c}}$ in Eq. (2) is the initially produced J/ψ and $c\bar{c}$ pair in heavy ion collisions. We calculated these quantities by using the Glauber model per event as follows:

$$N_{J/\psi}(\tau_0,b) = \sigma^{NN}_{J/\psi} T_{AA}(b), \tag{14}$$

where $T_{AA}(b)$ is nuclear overlap function, its impact-parameter-dependent (b dependent) values are taken from Ref. [44]. $\sigma^{NN}_{J/\psi}$ is the cross section for production in $p + p$ collision and its values for RHIC at $\sqrt{s} = 200$ GeV and for LHC at $\sqrt{s} = 2.76$ TeV are given in Table I. Similarly, we have calculated $N_{c\bar{c}}$ from the Glauber model:

$$N_{c\bar{c}}(b) = \sigma^{NN}_{c\bar{c}} T_{AA}, \tag{15}$$

where $\sigma^{NN}_{c\bar{c}}$ is the cross section for $c\bar{c}$ pair production in $p + p$ collisions. The $\sigma^{NN}_{c\bar{c}}$ has been calculated by using the pQCD approach for the GRV HO hadronic structure function [34], we obtained $\sigma^{NN}_{c\bar{c}} = 3.546$ mb for LHC at $\sqrt{s} = 2.76$ TeV and $\sigma^{NN}_{c\bar{c}} = 0.346$ mb for RHIC at $\sqrt{s} = 200$ GeV. The quantity

TABLE I. All cross sections are in units of millibarn (mb).

	$\sigma^{NN}_{J/\psi}$	$\sigma^{NN}_{\chi_c}$	$\sigma^{NN}_{\psi'}$
LHC	0.0072 [45]	$1.0\sigma^{NN}_{J/\psi}$	$0.30\sigma^{NN}_{J/\psi}$
RHIC	0.00139 [45]	$1.0\sigma^{NN}_{J/\psi}$	$0.30\sigma^{NN}_{J/\psi}$

$V(\tau)$ is the volume as a function of time τ. It is based on the QPM EOS of QGP and the isentropic evolution of QGP [40] and is given by

$$V(\tau,b) = v_0(b)\left(\frac{\tau_0}{\tau}\right)^{\left(\frac{1}{R}-1\right)}, \tag{16}$$

where R is the Reynolds number [40] and $v_0(b)$ is the initial volume at time τ_0, which is given as $v_0(b) = \pi(r_t - b/2)^2\tau_0$, where r_t is the radius of the fireball created.

Here we use a cooling law for temperature which not only depends on proper time (τ) but also varies with respect to number of participants ($N_{\rm part}$). The cooling law for temperature which connects proper time and $N_{\rm part}$ to the temperature of the system is as follows [39]:

$$T(\tau) = T_c\left(\frac{N_{\rm part}(\beta)}{N_{\rm part}(\beta_0)}\right)^{1/3}\left(\frac{\tau_{\rm QGP}}{\tau}\right)^{1/3}, \tag{17}$$

where $N_{\rm part}(\beta_0)$ is the number of participant corresponding to the most central bin β_0 as used in our calculation and $N_{\rm part}(\beta)$ is the number of participants corresponding to the bin β at which we want to calculate the temperature. $\tau_{\rm QGP}$ is the lifetime of QGP.

D. Cold-nuclear-matter effect

We have already discussed shadowing, absorption, and the Cronin effect as the three main nuclear effects on charmonium production. Nuclear absorption and the Cronin effect are not included in our calculation. We incorporate shadowing as the only dominant CNM effect in the current work.

Shadowing effect

We have used the EPS09 parametrization to obtain the shadowing for nuclei, with atomic mass number A, momentum fraction x, and scale μ, $S^i(A, x, \mu)$ [46,47]. The spatial variation of shadowing can be given in terms of shadowing and the nucleon density $\rho_A(r,z)$ as follows:

$$S^i_\rho(A,x,\mu,r,z) = 1 + N_\rho[S^i(A,x,\mu) - 1]\frac{\int dz\rho_A(r,z)}{\int dz\rho_A(0,z)}, \tag{18}$$

where N_ρ is determined by the following normalization condition [39]:

$$\frac{1}{A}\int d^2r dz\rho_A(s)S^i_\rho(A,x,\mu,r,z) = S^i(A,x,\mu). \tag{19}$$

The suppression factor due to shadowing is defined as

$$S_{sh} = R_{AA}(b) = \frac{d\sigma_{AA}/dy}{T_{AA}d\sigma_{pp}/dy}. \tag{20}$$

As mentioned in Ref. [48], the color-evaporation model gives σ_{AA} and σ_{pp} as follows:

$$\sigma_{AA} = \int dz_1 dz_2 d^2r dx_1 dx_2 \big[f_g^i(A,x_1,\mu,r,z_1) \times f_g^j(A,x_2,\mu,b-r,z_2)\sigma_{gg\to Q\bar{Q}}(x_1,x_2,\mu)\big], \quad (21)$$

$$\sigma_{pp} = \int dx_1 dx_2 [f_g(p,x_1,\mu) f_g(p,x_2,\mu) \times \sigma_{gg\to Q\bar{Q}}(x_1,x_2,\mu)]. \quad (22)$$

Here, x_1 and x_2 are the momentum fraction of the gluons in the two nuclei and they are related to the rapidity [39]. The superscripts i and j refer to the projectile and target nuclei, respectively.

The function $f_g^i(A,\ x,\ \mu,\ r,\ z_1)$ is determined from the gluon distribution function for proton $f_g(p,\ x,\ \mu)$ by using the following relations:

(1) $f_g^i(A,x_1,\mu,r,z_1) = \rho_A(s) S^i(A,x_1,\mu,r,z) f_g(p,x_1,\mu)$.

(2) $f_g^j(A,x_2,\mu,b-r,z_2) = \rho_A(s) S^j(A,x_2,\mu,b-r,z) f_g(p,x_2,\mu)$.

The value of the gluon distribution function $f_g(p,x,\mu)$ in a proton (indicated by label p) has been estimated by using CTEQ6 [49].

E. Color screening

We treat color screening as independent suppression mechanism acting until formation of charmonium bound states followed by gluonic dissociation along with the collisional damping. The original color-screening mechanisms [50] have been modified by Mishra *et al.* [51]. In our present work we have used quasiparticle model (QPM) equation-of-state-based model in which the pressure profile [40] and the cooling law of pressure are the main ingredients. The cooling law of pressure is given by

$$p(\tau,r) = A + \frac{B}{\tau^q} + \frac{C}{\tau} + \frac{D}{\tau^{c_s^2}}, \quad (23)$$

where $A = -c_1$, $B = c_2 c_s^2$, $C = \frac{4\eta q}{3(c_s^2-1)}$, and $D = c_3$, where c_1, c_2, c_3 are constants and have been calculated [40,41] by using different boundary conditions on energy density and pressure. Determining the pressure profile at initial time $\tau = \tau_i$ and at screening time $\tau = \tau_s$ we get

$$p(\tau_i,r) = A + \frac{B}{\tau_i^q} + \frac{C}{\tau_i} + \frac{D}{\tau_i^{c_s^2}} = p(\tau_i,0)h(r), \quad (24)$$

$$p(\tau_s,r) = A + \frac{B}{\tau_s^q} + \frac{C}{\tau_s} + \frac{D}{\tau_s^{c_s^2}} = p_{\rm QGP}, \quad (25)$$

where $p_{\rm QGP}$ is the pressure of QGP inside the screening region, required to dissociate J/ψ, as determined by QPM EOS of QGP [40,41]. After combining cooling law and pressure profile and equating screening time to the dilated formation time, we determined the radius of screening region r_s.

Assume that $c\bar{c}$ is formed inside the screening region at a point whose position vector is $\vec{r}$. It moves with transverse momentum p_T making an azimuthal angle ϕ (angle between the transverse momentum and position vector $r_{J/\psi}$). Then the condition for escape of $c\bar{c}$ without forming the charmonium states is expressed as

$$\cos\phi \geqslant Y, \quad Y = \frac{(r_s^2 - r_{J/\psi}^2)m - \tau_F^2 p_T^2/m}{2 r_{J/\psi}\tau_F p_T}, \quad (26)$$

where $r_{J/\psi}$ is the position vector at which the charm-anticharm quark pair is formed, τ_F is the proper formation time required for the formation of bound states of $c\bar{c}$ from correlated $c\bar{c}$ pairs, and m is the mass of charmonia ($m = M_{J/\psi}$, M_{χ_c}, $M_{\psi'}$ for different resonance states of charmonium).

Survival probability

In the color-screening scenario, the survival probability of charmonia in QGP medium can be expressed as

$$S_c(p_T,N_{\rm part}) = \frac{2(\alpha+1)}{\pi R_T^2}\int_0^{R_T} dr r \phi_{\max}(r)\left\{1 - \frac{r^2}{R_T^2}\right\}^\alpha, \quad (27)$$

where $\alpha = 0.5$ [50,51].

The condition on azimuthal angle $\phi_{\max}$ given by Eq. (4) is expressed as

$$\phi_{\max}(r) = \begin{cases} \pi & \text{if} \quad Y \leqslant -1 \\ \pi - \cos^{-1}|Y| & \text{if} \quad 0 \geqslant Y \geqslant -1 \\ \cos^{-1}|Y| & \text{if} \quad 0 \leqslant Y \leqslant -1 \\ 0 & \text{if} \quad Y \geqslant 1. \end{cases} \quad (28)$$

Then we have obtained the p_T-integrated survival probability in the color-screening scenario, which is given as [40,41]

$$S_c(N_{\rm part}) = \frac{\int_{p_{T\min}}^{p_{T\max}} S(p_T,N_{\rm part}) dp_T}{\int_{p_{T\min}}^{p_{T\max}} dp_T}, \quad (29)$$

for J/ψ, χ_c, and ψ' denoted by $S_c^{J/\psi}$, $S_c^{\chi_c}$, and $S_c^{\psi'}$, respectively. The range of p_T values used here is allowed by the corresponding experimental data.

F. Net survival probability

The initial J/ψ production after doing the shadowing correction is as follows:

$$N_{J/\psi}^i(\tau_0,b) = N_{J/\psi}(\tau_0,b) S_{sh}. \quad (30)$$

In Eq. (2), we replaced $N_{J/\psi}(\tau_0,\ b)$ with $N_{J/\psi}^i(\tau_0,b)$ from Eq. (30) and re-obtained Eq. (2) as follows:

$$N_{J/\psi}^f(\tau_f,b) = \epsilon(\tau_f)\left[N_{J/\psi}^i(\tau_0,b) + N_{c\bar{c}}^2 \int_{\tau_0}^{\tau_f} \times \Gamma_{F,nl}[V(\tau)\epsilon(\tau)]^{-1} d\tau \right]. \quad (31)$$

Now the survival probability due to shadowing and gluonic dissociation along with collisional damping can be written as

$$S_g^{J/\psi} = \frac{N_{J/\psi}^f(\tau_f,b)}{N_{J/\psi}(\tau_0,b)}. \quad (32)$$

In this model we assumed that, at initial stage of the QGP, the color screening would be dominated independent of the

gluonic dissociation but, at later stage, it would partially affect the J/ψ formation and can be coupled with gluonic dissociation. So we incorporate the color screening at the initial stage of QGP followed by gluonic dissociation along with the collisional damping, including shadowing. We express the survival probability by using Eqs. (29) and (32):

$$S_f^{J/\psi} = S_c^{J/\psi} S_g^{J/\psi}. \tag{33}$$

In the same way we calculated the survival probability for χ_c and $\psi^{'}$, written as, $S_f^{\chi_c}$ and $S_f^{\psi^{'}}$, respectively.

It has been observed that only 60% of J/ψ comes up by direct production whereas 30% is from the decay of χ_c and 10% is from the decay of $\psi^{'}$, so the net survival probability $S_{J/\psi}$ of a mixed system after incorporating feed-down is given as

$$S_{J/\psi} = \frac{0.60N_{J/\psi}S_f^{J/\psi} + 0.30N_{\chi_c}S_f^{\chi_c} + 0.10N_{\psi^{'}}S_f^{\psi^{'}}}{0.60N_{J/\psi} + 0.30N_{\chi_c} + 0.10N_{\psi^{'}}}. \tag{34}$$

III. RESULTS AND DISCUSSIONS

Before going into our results, we want to state that some short-hand notations have been used by us to show the different physical processes in the plots. We have used GD for gluonic dissociation, CD for collisional damping, CS for color screening, S for shadowing as a CNM effect, FD for the feed-down correction, and R for the regeneration via recombination of c and $\bar{c}$ quarks.

Figure 4 depicts our prediction on suppression (in terms of p_T integrated survival probability, S_p) of J/ψ in the QGP medium formed at RHIC as a function of $N_{\rm part}$ at midrapidity arising due to gluonic dissociation and collisional damping with and without shadowing as a CNM effect. The experimental data on J/ψ suppression obtained from the PHENIX experiment at RHIC [5] at the center-of-mass energy $\sqrt{s_{NN}} = 200$ GeV are also shown on the same graph for comparison with our predicted results. It is obvious from this figure that our result underpredicts the observed J/ψ suppression data without including shadowing. However, after including shadowing, it captures the experimental data on suppression reasonably well. In Fig. 5, we plot the survival probability versus $N_{\rm part}$ after including color screening along with the gluonic dissociation and collisional damping with and without the shadowing effect. Our predicted result is almost similar to that shown in Fig. 4 since color screening only affects higher charmonium states at RHIC energies. In Fig. 6, we plot the variation-of-recombination factor at RHIC energies versus $N_{\rm part}$. This graph indicates that, at RHIC energies, recombination for J/ψ increases very slowly with $N_{\rm part}$ and reaches to slightly greater than unity at the most central collisions. All the above-mentioned suppression (GD + CD + CS + S) along with the recombination are also

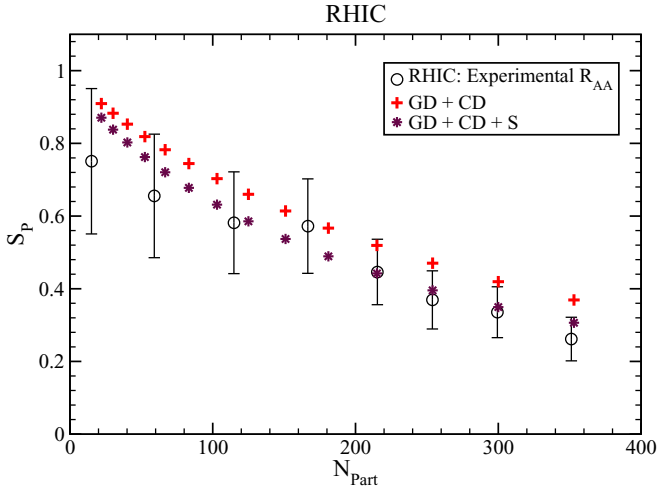

FIG. 4. (Color online) Survival probability (S_p) of J/ψ in a QGP medium versus $N_{\rm part}$ including gluonic dissociation (GD) and collisional damping (CD) at RHIC energies with and without shadowing effect (S).

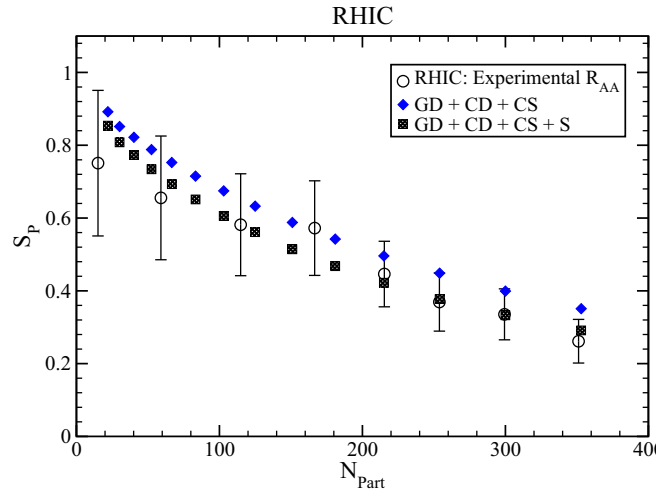

FIG. 5. (Color online) Survival probability versus $N_{\rm part}$ with gluonic dissociation (GD) and collisional damping (CD) along with color screening (CS) at RHIC energies with and without shadowing effect (S).

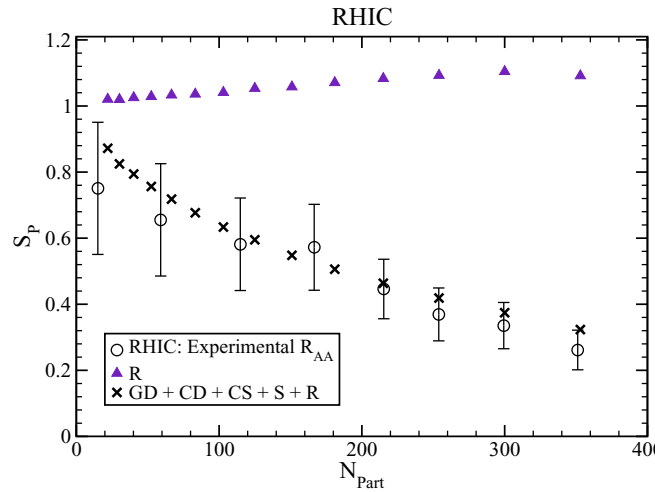

FIG. 6. (Color online) Same as Fig. 5 but the recombination effect (R) is also included. Only recombination (R) is also shown here.

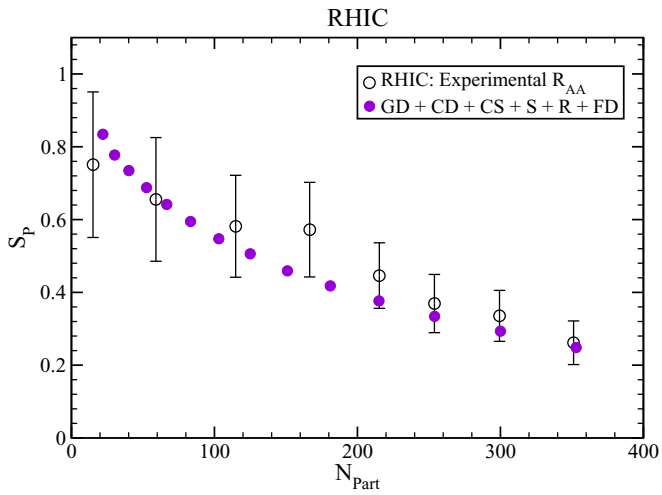

FIG. 7. (Color online) Same as Fig. 6 but feed-down (FD) due to higher resonances; namely, χ_c and $\psi^{'}$, is also included.

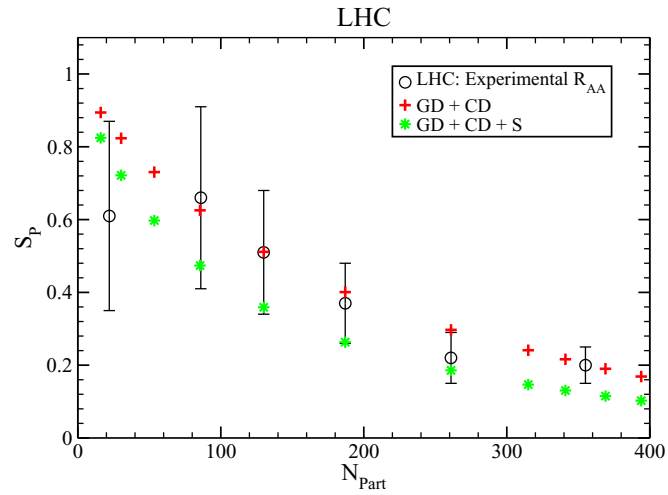

FIG. 8. (Color online) Survival probability (S_p) of J/ψ in QGP medium versus $N_{\rm part}$ including gluonic dissociation (GD) and collisional damping (CD) at LHC energies with and without shadowing effect (S).

plotted on the same graph which obviously will be nearly identical to the variation shown in Fig. 5 since the recombination factor turns out to be small even with the higher recombination reactivity at RHIC as compared with that of the LHC. This trend of reactivity is due to the low initial momentum of c and $\bar{c}$ quarks (contrary to what happens at LHC due to high initial momentum) which participate in the secondary charmonium formation at RHIC energies. Furthermore, the recombination is mainly governed by the number of $c\bar{c}$ pairs produced initially and by the reactivity of the uncorrelated c and $\bar{c}$ pair. Due to fewer $c\bar{c}$ pairs produced during the initial stage of collisions at RHIC energies and its quadratic dependence on $N_{c\bar{c}}$, the recombination is found to be small even with significant recombination reactivity at RHIC energies. So far, we have not included feed-down due to the decay of higher resonances of charmonium; namely, χ_c and $\psi^{'}$ to J/ψ. Therefore, the survival probability of J/ψ with contributions coming from all the suppression mechanisms (GD + CD + CS + S) mentioned above along with the recombination and feed-down via the decay of χ_c and $\psi^{'}$ to J/ψ is plotted with respect to $N_{\rm part}$ in Fig. 7. After including the feed-down due to higher charmonium resonances, J/ψ suppression increases at all centralities at RHIC energies but is still within experimental error bars. Thus, our results agree reasonably well with the suppression data at midrapidity obtained from the PHENIX experiment at RHIC at the center-of-mass energy $\sqrt{s_{NN}} = 200$ GeV.

Figure 8 shows J/ψ suppression at midrapidity versus $N_{\rm part}$ due to the gluonic dissociation and collisional damping with and without shadowing as a CNM effect. The experimental data on J/ψ suppression at midrapidity obtained from the CMS experiment at LHC [6] center-of-mass energy $\sqrt{s_{NN}} =$ 2.76 TeV are also depicted on the same graph for comparison. Our result without shadowing shows good agreement with the experimental data while, with the shadowing effect, it overpredicts the suppression. Figure 9 includes color screening with the above suppression contributions; namely, gluonic dissociation and collisional damping with and without the shadowing effect. This figure implies that our predicted result captures data without inclusion of the shadowing effect. While with the shadowing effect, it shows over suppression. The regeneration factor due to recombination of uncorrelated c and $\bar{c}$ pairs at LHC energies and feed-down via decay of higher resonances are two important phenomena which need to be incorporated to explain the data. Therefore, in the next two figures, we plot the above recombination effect with all the above-mentioned suppression mechanisms (GD + CD + CS + S) with and without feed-down arising due to higher-resonance states of the charmonium. Figure 10 presents all the above suppression contributions and the regeneration factor without including the feed-down effect due to higher resonances. Only recombination is also presented on the same

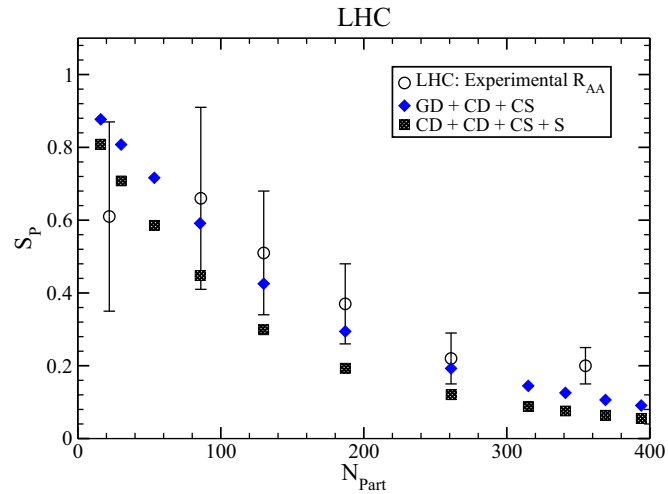

FIG. 9. (Color online) Survival probability versus $N_{\rm part}$ with gluonic dissociation (GD) and collisional damping (CD) along with color screening (CS) at LHC energies with and without shadowing effect (S).

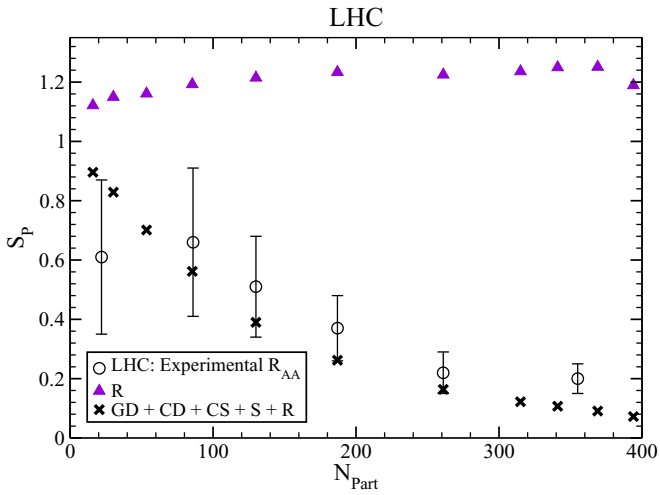

FIG. 10. (Color online) Same as Fig. 9 but recombination effect (R) is also included. Only recombination (R) is also shown here.

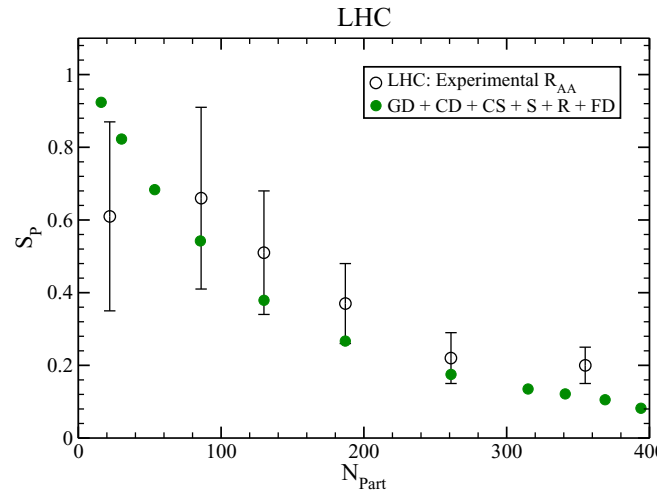

FIG. 11. (Color online) Same as Fig. 10 but feed-down (FD) due to higher resonances; namely, χ_c and $\psi^{'}$ are also included.

plot. This figure indicates that recombination of uncorrelated $c\bar{c}$ pairs at LHC energies varies from around 1.1 at the most peripheral to around 1.3 at the most central collisions. Comparatively larger recombination occurs here due to the sizable number of $c\bar{c}$ pairs produced at the LHC even with lower recombination reactivity. This figure clearly indicates that our predicted results capture the trend of data spanning over almost the whole range of $N_{\rm part}$. However, it depicts a slight over suppression almost at all centralities.

From Fig. 10 it is also evident that, at LHC energies, recombination begins to decrease beyond a certain value of $N_{\rm part}$ in contrast to the expectation based on its quadratic dependence on $N_{c\bar{c}}$ pairs and on volume $V(\tau)$. In fact, recombination has a somewhat complex dependence since it not only depends on the $N_{c\bar{c}}$ and $V(\tau)$ but also on the recombination reactivity Γ_F of uncorrelated c and $\bar{c}$ which further depends on the temperature of the medium and the momentum of c and $\bar{c}$. The decrease of the recombination factor at the highest $N_{\rm part}$, i.e., at the most central collision may be due to the peak value of Γ_F occurring at comparatively lower temperature (than at RHIC energies) and at a significantly small value at the highest $N_{\rm part}$. The temperature corresponding to that of $N_{\rm part}$ at LHC is too large and, at that much higher temperature, the value of Γ_F becomes very small (as can be seen from Fig. 3). That is why even with the highest value of $N_{c\bar{c}}$ at the most central collisions at LHC energies, the small and the reducing trend of Γ_F with temperature gives the overall decreasing behavior to the recombination factor. One can observe from Fig. 6 that the recombination factor at RHIC does not depict this kind of diminishing trend at the most central collisions. This is because the corresponding Γ_F value remains significantly large at RHIC (see Fig. 3) even at the most central collisions (at high temperatures). Thus there is no reducing trend in the recombination factor at the most central collisions at RHIC unlike at LHC energies. Despite of the above facts, the recombination factor at LHC is always higher than the corresponding value at RHIC energies for each centrality class (comparison between Figs. 6 and 10) which shows the dominance of $N^2_{c\bar{c}}$ dependence.

Figure 11 depicts our results for survival probability of J/ψ with respect to centrality after including contributions from all the suppression mechanisms (GD + CD + CS + S) as a function of $N_{\rm part}$ along with the recombination and feed-down due to decay of higher charmonium resonance states to J/ψ. Comparison of Figs. 10 and 11 shows that feed-down due to the decay of higher charmonium states to J/ψ increases the suppression a little bit at LHC energies and slightly overpredicts the suppression. However, it still depicts reasonable agreement with the data at LHC energies under the experimental uncertainties. Thus, our analysis shows that the current unified-model approach based on the combination of commonly employed suppression and recombination effects presents reasonably good agreement with the experimental data at RHIC and LHC energies over the whole range of centrality.

IV. CONCLUSIONS

In conclusion, we explained recent J/ψ suppression data at midrapidity obtained from RHIC and LHC experiments by using a common formulation based on Debye color screening, gluonic dissociation, and collisional damping (popularly called Landau damping in the literature) along with the recombination of uncorrelated c and $\bar{c}$ pairs in the later stage of QGP formation. Shadowing of parton distribution as a CNM effect determined by the Vogt approach and feed-down due to decay of higher resonances of charmonium have also been included in the current work. The recombination effect is incorporated via a transport approach by using two self-coupled transport equations. The QGP medium is assumed to be expanding under Bjorken's scaling law at midrapidity. Our current model based on the combination of color screening, gluonic dissociation, along with collisional damping plus the recombination effect explain J/ψ suppression data obtained from both the energies reasonably well without introducing any extra parameter

while moving from one set of data at one energy to another set of data at the other energy. The explanation of two different sets of suppression data at two different energies, differing by few orders of magnitude, employing a single set of mechanisms without including any new parameter, adds importance to our current approach. It is also clear from our results that J/ψ suppression in QGP medium is a result of many complex suppression mechanisms contrary to a single mechanism. Recombination is also important to include to explain charmonium suppression, especially at LHC energies. Note that, although there are few parameters in our current formulation, not even a single parameter is varied freely to explain the suppression data. We have taken all parameter values based on earlier works.

ACKNOWLEDGMENTS

P.K.S. is thankful to Council of Scientific and Industrial Research, Government of India for financial assistance. One of the authors (S.G.) acknowledges Broadcom India Research Pvt. Ltd. for allowing the use of its computational resources required for this work. C.R.S. and M.M. are grateful to the Department of Science and Technology, New Delhi for financial assistance.

[1] N. Brambilla *et al.*, Eur. Phys. J. C **71**, 1534 (2011).
[2] T. Matsui and H. Satz, Phys. Lett. B **178**, 416 (1986).
[3] M. C. Abreu *et al.* (NA50 Collaboration), Phys. Lett. B **477**, 28 (2000); B. Alessandro *et al.* (NA50 Collaboration), Eur. Phys. J. C **39**, 335 (2005).
[4] R. Arnaldi *et al.* (NA60 Collaboration), Phys. Rev. Lett. **99**, 132302 (2007).
[5] A. Adare *et al.* (PHENIX Collaboration), Phys. Rev. Lett. **98**, 232301 (2007).
[6] S. Chatrchyan *et al.* (CMS Collaboration), J. High Energy Phys. 05 (2012) 063.
[7] B. Abelev *et al.* (ALICE Collaboration), Phys. Rev. Lett. **109**, 072301 (2012).
[8] A. Adare *et al.* (PHENIX Collaboration), Phys. Rev. Lett. **112**, 252301 (2014).
[9] M. Laine, O. Philipsen, P. Romatschke, and M. Tassler, JHEP 03 (2007) 054.
[10] L. Thakur, U. Kakade, and B. K. Patra, Phys. Rev. D **89**, 094020 (2014).
[11] N. Brambilla, J. Ghiglieri, A. Vairo, and P. Petreczky, Phys. Rev. D **78**, 014017 (2008).
[12] C. Y. Wong, Phys. Rev. C **72**, 034906 (2005); Y. Park, K. I. Kim, T. Song, S. H. Lee, and C. Y. Wong, *ibid.* **76**, 044907 (2007).
[13] M. E. Peskin, Nucl. Phys. B **156**, 365 (1979).
[14] G. Bhanot and M. E. Peskin, Nucl. Phys. B **156**, 391 (1979).
[15] G. T. Bodwin, arXiv:1208.5506.
[16] H. Satz, Acta Phys. Pol. B Proc. Suppl. **7**, 49 (2014).
[17] G. T. Bodwin, E. Braaten, and G. P. Lepage, Phys. Rev. D **51**, 1125 (1995); **55**, 5853 (1997).
[18] G. T. Bodwin, Int. J. Mod. Phys. Conf. Ser. **02**, 9 (2011).
[19] Z.-B. Kang, J.-W. Qiu, and G. Sterman, Phys. Rev. Lett. **108**, 102002 (2012).
[20] Z.-B. Kang, Y.-Q. Ma, J.-W. Qiu, and G. Sterman, Phys. Rev. D **90**, 034006 (2014).
[21] S. P. Baranov, Phys. Rev. D **66**, 114003 (2002).
[22] S. P. Baranov and A. Szczurek, Phys. Rev. D **77**, 054016 (2008).
[23] K. Zhou, N. Xu, Z. Xu, and P. Zhuang, Phys. Rev. C **89**, 054911 (2014).
[24] A. H. Muller and J. W. Qin, Nucl. Phys. B **268**, 427 (1986).
[25] J. W. Cronin *et al.*, Phys. Rev. D **11**, 3105 (1975).
[26] J. Hufner, Y. Kurihara, and H. J. Pirner, Phys. Lett. B **215**, 218 (1988).
[27] C. Gerschel and J. Hufner, Phys. Lett. B **207**, 253 (1988).
[28] C. Lourenco, R. Vogt, and H. K. Wohri, JHEP 02 (2009) 014.
[29] P. Braun-Munzinger and J. Stachel, Phys. Lett. B **490**, 196 (2000); P. Braun–Munzinger and J. Stachel, Nucl. Phys. A **690**, 119 (2001).
[30] A. Andronic, P. Braun-Munzinger, K. Redlich, and J. Stachel, Phys. Lett. B **571**, 36 (2003); **652**, 259 (2007).
[31] L. Grandchamp and R. Rapp, Nucl. Phys. A **709**, 415 (2002).
[32] L. Grandchamp, R. Rapp, and G. E. Brown, Phys. Rev. Lett. **92**, 212301 (2004).
[33] R. L. Thews, M. Schroedter, and J. Rafelski, Phys. Rev. C **63**, 054905 (2001).
[34] R. L. Thews, Eur. Phys. J. C **43**, 97 (2005); Nucl. Phys. A **702**, 341 (2002).
[35] R. L. Thews and M. L. Mangano, Phys. Rev. C **73**, 014904 (2006).
[36] B. Zhang, C. M. Ko, B. A. Li, Z. W. Lin, and S. Pal, Phys. Rev. C **65**, 054909 (2002).
[37] E. L. Bratkovskaya, W. Cassing, and H. Stocker, Phys. Rev. C **67**, 054905 (2003).
[38] F. Nendzig and G. Wolschin, Phys. Rev. C **87**, 024911 (2013).
[39] S. Ganesh and M. Mishra, Phys. Rev. C **88**, 044908 (2013); **91**, 034901 (2015).
[40] P. K. Srivastava, M. Mishra, and C. P. Singh, Phys. Rev. C **87**, 034903 (2013).
[41] P. K. Srivastava, S. K. Tiwari, and C. P. Singh, Phys. Rev. C **88**, 044902 (2013).
[42] H. Satz, J. Phys. G **32**, 25(R) (2006).
[43] D. Pal, A. Sen, M. G. Mustafa, and D. K. Srivastava, Phys. Rev. C **65**, 034901 (2002).
[44] G. Aad *et al.* (ATLAS Collaboration), Phys. Rev. Lett. **114**, 072302 (2015).
[45] T. Song, K. C. Han, and C. M. Ko, Phys. Rev. C **84**, 039902 (2011).
[46] R. Vogt, Phys. Rev. C **81**, 044903 (2010).
[47] K. J. Eskola, H. Paukkunen, and C. A. Salgado, JHEP 04 (2009) 065.
[48] V. Emelyanov, A. Khodinov, S. R. Klein, and R. Vogt, Phys. Rev. Lett. **81**, 1801 (1998).
[49] J. Pumplin, D. R. Stump, J. Huston, H. L. Lai, P. M. Nadolsky, and W. K. Tung, JHEP 07 (2002) 012.
[50] M.-C. Chu and T. Matsui, Phys. Rev. D **37**, 1851 (1988).
[51] M. Mishra, C. P. Singh, V. J. Menon, and R. K. Dubey, Phys. Lett. B **656**, 45 (2007).